

Two dimensional time-dependent creep analysis of a thick-walled FG cylinder based on first order shear deformation theory

Abbas Loghman^{*}, Reza K. Faegh^a and Mohammad Arefi^b

Department of Solid Mechanic, Faculty of Mechanical Engineering, University of Kashan, Kashan 87317-51167, Iran

(Received July 29, 2017, Revised December 4, 2017, Accepted December 5, 2017)

Abstract. In this paper the time-dependent creep analysis of a thick-walled FG cylinder with finite length subjected to axisymmetric mechanical and thermal loads are presented. First order shear deformation theory (FSDT) is used for description of displacement components. Inner and outer temperatures and outer pressure are considered as thermo-mechanical loadings. Both thermal and mechanical loadings are assumed variable along the axial direction using the sinusoidal distribution. To find temperature distribution, two dimensional heat transfer equation is solved using the required boundary conditions. The energy method and Euler equations are employed to reach final governing equations of the cylinder. After determination of elastic stresses and strains, the creep analysis can be performed based on the Yang method. The results of this research indicate that the boundaries have important effects on the responses of the cylinder. The effect of important parameters of this analysis such as variable loading, non-homogeneous index of functionally graded materials and time of creep is studied on the behaviors of the cylinder.

Keywords: creep analysis; first order shear deformation theory; functionally graded materials; cylindrical shell

1. Introduction

Pressure vessels are extensively employed in different industries as chemical reactors, reservoir tanks and numerous other applications. When the pressure loadings are compounded with thermal loads, the creep analysis is required in long times. Creep analysis is including derivation of relations between history of stress and deformation and finally finding the damage due to creep and life assessment. Axi-symmetric one dimensional analysis of cylindrical pressure vessels made of isotropic material is one of the traditional problems which have been previously studied. In one dimensional analysis, the effect of end boundaries of cylinder is ignored. To account this case, a two dimensional analysis is required. Considering two dimensional loading and boundary conditions may be considered as new subjects in the context of mechanical engineering. Combination of pressure vessels, creep analysis and first order shear deformation theory in this paper leads to important issue. A literature review is presented to reflect necessity of this paper.

Elastic and Time-dependent creep stress analysis of FG cylindrical shell under axially constant loading has been investigated by various researchers. Sim and Penny (1971) incorporated the effects of initial elastic loading of thick-walled tubes followed by stress redistribution due to creep

process to a stationary stress state. Loading conditions was included internal pressure, external surface loading and inertia loading. Loghman and Wahab (1996) studied the creep stress and damage histories of thick-walled tubes using the material constant creep and creep rupture properties defined by the theta projection concept. Yang (2000) presented a solution for time-dependent creep behavior of FG cylinders. It was assumed that creep behavior can be modeled as the Norton's law. Using the Norton's law, equations of equilibrium, strain-displacement and stress-strain relations in the rate form incorporate with Prandtl-Reuss relations; a governing differential equation for the displacement rate has been derived. There was no exact solution for the derived differential equation and consequently, a numerical method has been provided based on assumption of the stress and strain rates. Mechanical stresses of functionally graded cylindrical and spherical shells were derived by Tutuncu and Ozturk (2001). The effect of material in homogeneity and mechanical loads was investigated on the results. Plane elasticity theory was used by Jabbari et al. (2002) to investigate thermo-elastic analysis of a functionally graded cylinder under thermal and mechanical loads. The used method and solution was applicable for FG cylindrical pressure vessels with infinite length. The effect of gradation of material properties as well as mechanical and thermal loadings has been studied in this paper. For solution of cylindrical pressure vessels with finite length, the effect of boundaries is appeared in the solution procedure. The both ends of cylindrical shells can change uniform distribution of displacement components and leads to shear strains and stresses. The shear stress cannot be calculated by the one dimensional symmetric plane elasticity theory used in mentioned reference.

*Corresponding author, Associate Professor,
E-mail: aloghman@kashanu.ac.ir

^a M.S., Master Student, E-mail: reza_faegh@hotmail.com

^b Assistant Professor,
E-mail: arefi@kashanu.ac.ir; arefi63@gmail.com

Rimrott *et al.* (1960) studied creep analysis of pressure vessels and time to rupture. Moosaie (2016) presented nonlinear thermo-elastic analysis of a FG thick-walled cylinder made of temperature dependent materials. Creep deformation and stresses in thick-walled FGM cylindrical vessels subjected to internal pressure was presented by You *et al.* (2007). They obtained a closed form solution for steady state creep stresses in FGM cylinders. Thermal stresses were not considered and stress redistributions were not presented. Jabbari *et al.* (2009) implemented a two-dimensional axisymmetric analysis via solving two-dimensional heat transfer differential equations analytically using the Bessel functions. They used a sinusoidal variation along the axial direction for description of radial and axial displacements. Due to type of chosen variation function, the proposed solution was only applicable for simply supported short cylinders. Loghman and Shokouhi (2009) investigated creep stress redistribution and damage histories of thick-walled spheres using the theta projection concept and loading conditions. Although intensive investigation considering creep of thick-walled cylinders and spheres with constant material properties can be found in the existing references, however, little publication can be found dealing with time-dependent creep of FGM cylinders. Loghman *et al.* (2010) studied the time-dependent creep in a thick-walled FGM cylinder under magneto-thermo-mechanical loading using initial elastic stresses at zero time and stress rates to obtain history of stresses. They found that radial stress redistribution is not significant but the circumferential and effective stresses experience major changes. Some literatures on the pressure vessels and shear deformation theory can be observed in references (Arefi and Rahimi 2010, 2014, Arefi *et al.* 2012, Kelesm and Conker 2011, Arefi and Rahimi (2012a, b), Rahimi *et al.* 2012, Khoshgoftar *et al.* 2013, Meziane *et al.* 2014, Yahia *et al.* 2015, Bounouara *et al.* 2016, Zemri *et al.* 2015, Bourada *et al.* 2015, Draiche *et al.* 2016). Bellifa *et al.* (2016) investigated on a new first-order shear deformation theory for bending and dynamic behaviors of functionally graded plates. Moreover, the number of unknowns of this theory was the least one comparing with the traditional first-order and the other higher order shear deformation theories Loghman *et al.* (2013) studied the effects of particle content; particle size, operating temperature and magnetic field on steady-state creep behavior of thick-walled rotating cylinders made of Al-SiC composites. It has been concluded that increasing particle size and operating temperature significantly increases the effective creep strain rates. It has also been illustrated that magnetic field decreases the stresses and the effective creep strain rates. Kheirkhah and Loghman (2015) studied the stresses and electric potential redistributions of a cylinder made from functionally graded piezoelectric material (FGPM). All the mechanical, thermal and piezoelectric properties were modeled based on power-law distribution of volume fraction. A semi-analytical method in conjunction with the Mendelson method of successive approximation was therefore proposed for this analysis. The effect of Pasternak foundation was investigated on the two dimensional thermo-elastic analysis of a functionally graded cylinder subjected to constant mechanical and thermal loadings by Arefi *et al.* (2016a).

Application of first order shear deformation theory for functionally graded piezoelectric cylinder was performed by Arefi and Rahimi (2012a, b, c). Brnic *et al.* (2016) studied some mechanical, creep and fatigue properties of low alloy 42CrMo4 steel at different temperatures. Sahan (2015) presented an alternative analytical method for transient vibration analysis of doubly-curved laminated shells subjected to dynamic loads. Many studies on the analysis of the thermal behavior of FGM and using various degrees of shear deformation theory can be observed in references (Mouffoki *et al.* 2017, Boudarba *et al.* 2013, 2016, Bousahla *et al.* 2016, Hamidi *et al.* 2015, Beldjelili *et al.* 2016, Abdelbaki *et al.* 2017, El-Haina *et al.* 2017). The influence of thermal loads was studied on the elastic behaviors of cylindrical shell and sandwich plates (Arefi *et al.* 2016b, Arefi and Zenkour 2017a, Zenkour and Arefi 2017). Some linear and nonlinear analysis of functionally graded structures was studied in detail to capture influence of in-homogeneous index on the elastic results (Arefi and Rahimi 2011, 2012c, Arefi *et al.* 2011, Arefi and Khoshgoftar 2014, Arefi 2014, Mohammadimehr *et al.* 2016). Loghman *et al.* (2017) studied nonsymmetric analysis of FG cylinder subjected to thermal and mechanical loads. Arefi and Bidgoli (2017) presented an analytical work about two dimensional thermo-elastic analysis of axially variable pressure cylindrical shell. Arefi *et al.* (2016c) presented free vibration analysis of laminated cylindrical shell. Sinusoidal shear deformation theory was used by Arefi and Zenkour (2016, 2017b) for transient and static analyses of sandwich nano plates.

A comprehensive literature review was performed in Introduction. One can conclude that although some theoretical works on the creep analyses of cylindrical pressure vessels were presented however it is proved that there is no published work about two dimensional thermo-elastic creep analysis of cylindrical pressure vessels based on first order shear deformation theory. Our goal in this paper is to present two dimensional time-dependent creep analysis of a functionally graded cylinder subjected to longitudinally variable thermal and mechanical loads. First order shear deformation theory is used for description of two dimensional displacement components. Yang method and Norton's law are employed for time dependent creep analysis. The numerical results are presented to reflect the influences of important parameters such non-homogeneous index, time of creep, radial location of cylinder and thermal and mechanical loadings on the two dimensional time dependent responses of the cylinder.

2. Thermal analysis

Consider a clamped-clamped functionally graded hollow cylinder with finite length l , internal radius R_i and external radius R_o . Cylindrical coordinates (r, θ, x) are used in the analysis. Mechanical and thermal properties except Poisson's ratio are assumed variable along the thickness direction based on the simple power law variation as $E = E_0 r^\beta$ and $\alpha = \alpha_0 r^\beta$ (Keles and Tutuncu 2011). The following data for geometry and material properties (Loghman *et al.* 2010, Xuan *et al.* 2009, You *et al.* 2007, Dai and Fu 2007)

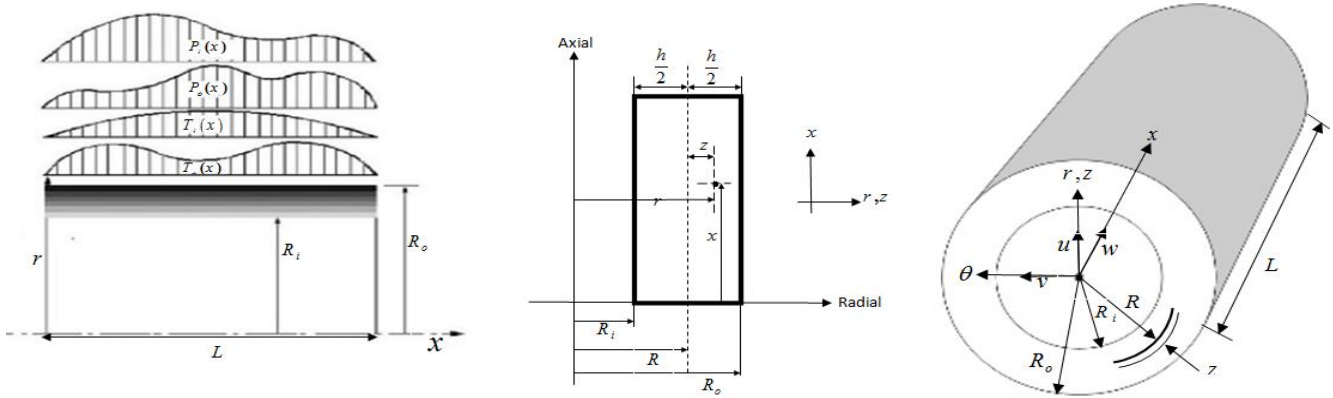


Fig. 1 The schematic of a cylindrical shell under axially variable temperature and pressure

are used in this paper as follows

$$\begin{aligned}
 R_i &= 0.4 \quad R_o = 0.6 \\
 E_0 &= 22GPa \quad \alpha_0 = 1.2 \times 10^{-6} \frac{1}{^\circ C} \\
 \nu &= 0.3 \quad \beta = -2, -1, 0, 1, 2 \\
 n_0 &= 3 \quad b_0 = 1.1 \times 10^{-36} \quad b_1 = -5
 \end{aligned}
 \tag{1}$$

The cylinder is subjected to axisymmetric steady-state temperature loads $T_i(x)$ on the inner surface and $T_o(x)$ on the outer surface. Temperatures on its two end surfaces are assumed zero. In addition, the internal pressure $P_i(x)$ and external pressure $P_o(x)$ are applied on the cylinder. Details of the functionally graded circular hollow cylinder are shown in Fig. 1.

In this stage and before performing the thermo-elastic analysis, temperature distribution should be determined. Heat conduction equation in cylindrical coordinate system is presented as follows (Jabbari *et al.* 2009)

$$\frac{1}{r} \frac{\partial}{\partial r} (kr \frac{\partial T}{\partial r}) + \frac{1}{r^2} \frac{\partial}{\partial \theta} (k \frac{\partial T}{\partial \theta}) + \frac{\partial}{\partial x} (k \frac{\partial T}{\partial x}) + \dot{q} = \rho c \frac{\partial T}{\partial t} \tag{2}$$

In which, T is temperature distribution, k is thermal conductivity, \dot{q} is heat generation, ρ is density, c is specific heat and (r, θ, x) are used coordinate described in Fig. 1.

For a cylinder without heat generation, symmetric steady state heat conduction and considering the power law distribution for material properties using relation $K(r) = K_0 r^{m_3}$, the two dimensional heat conduction relation is reduced to (Jabbari *et al.* 2009)

$$\frac{\partial^2 T}{\partial r^2} + (m_3 + 1) \frac{1}{r} \frac{\partial T}{\partial r} + \frac{\partial^2 T}{\partial x^2} = 0 \tag{3}$$

By employing the method of separation of variable and employing the solution as $T(r, x) = T(r) T(x)$, Eq. (3) is updated as

$$\frac{T''(x)}{T(x)} = -\lambda \tag{4}$$

$$\frac{T''(r)}{T(r)} + \frac{m_3 + 1}{r} \frac{T'(r)}{T(r)} = \lambda \tag{4}$$

General thermal boundary conditions of the cylinder are assumed as

$$\begin{cases} C_{11}T(a, x) + C_{12}T_{,r}(a, x) = f_1(x) \\ C_{21}T(b, x) + C_{22}T_{,r}(b, x) = f_2(x) \end{cases} \tag{5}$$

Regard to all states of constant λ for arriving to nontrivial solution present $\lambda = k^2$ and consequently yields solution as

$$T(x) = c_1 \sin(kx) + c_2 \cos(kx) \tag{6}$$

The other function of temperature distribution along the r direction yields following solution using Bessel functions as

$$T''(r) + \frac{m_3 + 1}{r} T'(r) - k^2 T(r) = 0 \rightarrow T(r) = r^{-\frac{m_3}{2}} [c_3 I_{\frac{m_3}{2}}(kr) + c_4 k_{\frac{m_3}{2}}(kr)] \tag{7}$$

In which $k = \frac{n\pi}{L} = \zeta_n$, $\frac{m_3}{2} = \beta$. Finally the two dimensional temperature distribution is derived as

$$T(r, x) = \sum_{n=1}^{\infty} r^{-\beta} [a_n I_{\beta}(\zeta_n r) + b_n k_{\beta}(\zeta_n r)] \sin(\frac{n\pi}{L} x) \tag{8}$$

By considering the homogeneous boundary condition at two ends of the cylinder and constant temperatures at inner and outer radii, we will have

$$\begin{cases} T(a, x) = f_1(x) = T_1(x) \\ T(b, x) = f_2(x) = T_2(x) \end{cases} \tag{9}$$

Imposing the mentioned boundary conditions present integration constants as follows

$$a_n = \frac{e_1 e_6 - e_2 e_4}{e_3 e_6 - e_4 e_5}, \quad b_n = \frac{e_2 e_3 - e_1 e_5}{e_3 e_6 - e_4 e_5} \tag{10}$$

In which, $e_i, i = 1..6$ are calculated as

$$\begin{aligned}
 e_1 &= \frac{2}{L} \int_0^L T_1(x) \sin\left(\frac{n\pi}{L}x\right) dx \\
 e_2 &= \frac{2}{L} \int_0^L T_2(x) \sin\left(\frac{n\pi}{L}x\right) dx \\
 e_3 &= a^{-\beta} I_\beta(\zeta_n a) \\
 e_4 &= a^{-\beta} k_\beta(\zeta_n a) \\
 e_5 &= b^{-\beta} I_\beta(\zeta_n a) \\
 e_6 &= b^{-\beta} k_\beta(\zeta_n a)
 \end{aligned}
 \tag{11}$$

3. Creep analysis based on FSDT formulation

Based on the first order shear deformation theory, displacement components are considered as linear combination of displacement of mid-surface and rotation about mid-surface. For a symmetric two dimensional analysis, displacement field is provided as Arefi and Rahimi (2012b)

$$\begin{Bmatrix} U_z(x, z) \\ W_x(x, z) \end{Bmatrix} = \begin{Bmatrix} u(x) \\ w(x) \end{Bmatrix} + z \begin{Bmatrix} \phi_r(x) \\ \phi_x(x) \end{Bmatrix}
 \tag{12}$$

In which, U_z, W_x are radial and axial displacements, u, w are displacements of mid-surface of cylinder and ϕ_r, ϕ_x are rotation components. Using the linear strain-displacement relations, normal and shear strain components are derived as

$$\begin{cases}
 \varepsilon_{zz} = \frac{\partial U_z}{\partial z} = \phi_z \\
 \varepsilon_{\theta\theta} = \frac{1}{r} \left(\frac{\partial U_\theta}{\partial \theta} + U_z \right) = \frac{u}{R+z} + z \frac{\phi_z}{R+z} \\
 \varepsilon_{xx} = \frac{\partial W_x}{\partial x} = \frac{\partial w}{\partial x} + z \frac{\partial \phi_x}{\partial x} \\
 \gamma_{z\theta} = 2 \times \varepsilon_{z\theta} = \frac{1}{r} \frac{\partial U_z}{\partial \theta} + \frac{\partial V_\theta}{\partial z} - \frac{V_\theta}{r} = 0 \\
 \gamma_{zx} = 2 \times \varepsilon_{zx} = \frac{\partial W_x}{\partial z} + \frac{\partial U_z}{\partial x} = \phi_x + \frac{\partial u}{\partial x} + z \frac{\partial \phi_x}{\partial x} \\
 \gamma_{x\theta} = 2 \times \varepsilon_{x\theta} = \frac{1}{r} \frac{\partial W_x}{\partial \theta} + \frac{\partial V_\theta}{\partial x} = 0
 \end{cases}
 \tag{13}$$

The three-dimensional stress-strain relations in cylindrical coordinate may be written as (Penny and Marriott 1971, Kraus 1980)

$$\begin{aligned}
 \sigma_{rr} &= \frac{E}{(1+\nu)(1-2\nu)} \left[\begin{aligned} &(1-\nu)\varepsilon_{rr} + \nu(\varepsilon_{\theta\theta} + \varepsilon_{xx}) - (1+\nu)\alpha T \\ &-(1-\nu)\varepsilon_{rr}^c - \nu(\varepsilon_{\theta\theta}^c + \varepsilon_{xx}^c) \end{aligned} \right] \\
 \sigma_{\theta\theta} &= \frac{E}{(1+\nu)(1-2\nu)} \left[\begin{aligned} &(1-\nu)\varepsilon_{\theta\theta} + \nu(\varepsilon_{rr} + \varepsilon_{xx}) - (1+\nu)\alpha T \\ &-(1-\nu)\varepsilon_{\theta\theta}^c - \nu(\varepsilon_{rr}^c + \varepsilon_{xx}^c) \end{aligned} \right] \\
 \sigma_{xx} &= \frac{E}{(1+\nu)(1-2\nu)} \left[\begin{aligned} &(1-\nu)\varepsilon_{xx} + \nu(\varepsilon_{rr} + \varepsilon_{\theta\theta}) - (1+\nu)\alpha T \\ &-(1-\nu)\varepsilon_{xx}^c - \nu(\varepsilon_{rr}^c + \varepsilon_{\theta\theta}^c) \end{aligned} \right]
 \end{aligned}
 \tag{14}$$

$$\tau_{rx} = K \frac{E}{1+\nu} \left[\frac{1}{2} \gamma_{rx} - \varepsilon_{rx}^c \right]
 \tag{14}$$

Using stress and strain components, strain energy per unit volume of the FG cylindrical shell is obtained as

$$\begin{aligned}
 \bar{u} &= \frac{1}{2} \{ \sigma_{rr} \varepsilon_{rr} + \sigma_{\theta\theta} \varepsilon_{\theta\theta} + \sigma_{xx} \varepsilon_{xx} + \tau_{rx} \varepsilon_{rx} \} \\
 \rightarrow \bar{u} &= \frac{1}{2} \frac{E}{(1+\nu)(1-2\nu)} \left[\begin{aligned} &(1-\nu)(\varepsilon_{rr}^2 + \varepsilon_{\theta\theta}^2 + \varepsilon_{xx}^2) \\ &+ 2\nu(\varepsilon_{rr} \varepsilon_{\theta\theta} + \varepsilon_{rr} \varepsilon_{xx} + \varepsilon_{\theta\theta} \varepsilon_{xx}) \\ &- (1+\nu)\alpha T (\varepsilon_{rr} + \varepsilon_{\theta\theta} + \varepsilon_{xx}) + K(1-2\nu) \left[\frac{1}{2} \gamma_{rx} - \varepsilon_{rx}^c \right] \gamma_{rx} \\ &- (1-\nu)(\varepsilon_{rr}^c \varepsilon_{rr} + \varepsilon_{\theta\theta}^c \varepsilon_{\theta\theta} + \varepsilon_{xx}^c \varepsilon_{xx}) \\ &- \nu(\varepsilon_{rr}^c (\varepsilon_{\theta\theta} + \varepsilon_{xx}) + \varepsilon_{\theta\theta}^c (\varepsilon_{rr} + \varepsilon_{xx}) + \varepsilon_{xx}^c (\varepsilon_{rr} + \varepsilon_{\theta\theta})) \end{aligned} \right]
 \end{aligned}
 \tag{15}$$

Substitution of strain components into strain energy per unit volume and integration over the volume of the structure, total strain energy of the cylinder is obtained as

$$\begin{aligned}
 U &= \pi \int_0^L \int_{-h/2}^{+h/2} \frac{E}{(1+\nu)(1-2\nu)} \left\{ \begin{aligned} &(1-\nu) \left[(R+z)\phi_z^2 + \frac{u^2}{R+z} + \frac{z^2 \phi_z^2}{R+z} \right. \\ &+ \left. \frac{2uz\phi_x}{R+z} + (R+z) \left[\left(\frac{\partial w}{\partial x} \right)^2 + z^2 \left(\frac{\partial \phi_x}{\partial x} \right)^2 + 2z \frac{\partial w}{\partial x} \frac{\partial \phi_x}{\partial x} \right] \right. \\ &+ 2\nu \left[u\phi_z + z\phi_z^2 + (R+z)\phi_z \frac{\partial w}{\partial x} + (R+z)z\phi_z \frac{\partial \phi_x}{\partial x} + u \frac{\partial w}{\partial x} \right. \\ &+ z u \frac{\partial \phi_x}{\partial x} + z\phi_z \frac{\partial w}{\partial x} + z^2 \phi_z \frac{\partial \phi_x}{\partial x} \left. \right] - (1+\nu)\alpha T \left[(R+z)\phi_z + u + z\phi_z \right. \\ &+ \left. (R+z) \frac{\partial w}{\partial x} + (R+z)z \frac{\partial \phi_x}{\partial x} \right] \\ &+ K \frac{(1-2\nu)(R+z)}{2} \left[\phi_x^2 + \left(\frac{\partial u}{\partial x} \right)^2 + z^2 \left(\frac{\partial \phi_x}{\partial x} \right)^2 \right] \\ &+ K(1-2\nu)(R+z) \left[\phi_x \frac{\partial u}{\partial x} + z\phi_x \frac{\partial \phi_z}{\partial x} + z \frac{\partial u}{\partial x} \frac{\partial \phi_z}{\partial x} \right] \\ &- K(1-2\nu)(R+z) \left[\varepsilon_{zx}^c \phi_x + \varepsilon_{zx}^c \frac{\partial u}{\partial x} + \varepsilon_{zx}^c z \frac{\partial \phi_z}{\partial x} \right] \\ &- (1-\nu) \left[(R+z)\varepsilon_{zz}^c \phi_z + \varepsilon_{\theta\theta}^c u + \varepsilon_{\theta\theta}^c z \phi_z + (R+z)\varepsilon_{xx}^c \frac{\partial w}{\partial x} \right. \\ &+ (R+z)\varepsilon_{xx}^c z \frac{\partial \phi_x}{\partial x} \left. \right] - \nu \left[\varepsilon_{zz}^c u + \varepsilon_{zz}^c z \phi_z + (R+z)\varepsilon_{zz}^c \frac{\partial w}{\partial x} \right. \\ &+ (R+z)\varepsilon_{zz}^c z \frac{\partial \phi_x}{\partial x} + (R+z)\varepsilon_{\theta\theta}^c \phi_z + (R+z)\varepsilon_{\theta\theta}^c \frac{\partial w}{\partial x} \\ &+ (R+z)\varepsilon_{\theta\theta}^c z \frac{\partial \phi_x}{\partial x} + (R+z)\varepsilon_{xx}^c \phi_z + \varepsilon_{xx}^c u + \varepsilon_{xx}^c z \phi_z \left. \right] \} dz dx
 \end{aligned}
 \tag{16}$$

In more simple form, the total energy is presented as combination of mechanical, thermal and creep energies as follows

$$\begin{aligned}
 U &= \int_0^L [U_s(x) - U_c(x) - U_{cr}(x)] dx \\
 U_s(x) &= \sum_{i=1}^9 A_i(x) f_i(x) \rightarrow f_i(x) = f_i(u, w, \phi_z, \phi_x) \\
 U_{cr}(x) &= \sum_{i=1}^9 B_i(x) g_i(x) \rightarrow g_i(x) = g_i(u, w, \phi_z, \phi_x)
 \end{aligned}
 \tag{17}$$

$$U_c(x) = \sum_{i=1}^9 C_i(x) j_i(x) \rightarrow j_i(x) = j_i(u, w, \phi_x, \phi_z) \quad (17)$$

In which, $A_i(x)$, $f_i(x)$, $B_i(x)$, $g_i(x)$, $C_i(x)$, $j_i(x)$ are functions of u , w , ϕ_x , ϕ_z and material properties. External energy due to inner and outer pressures is derived as

$$W = \int_0^L [d_1 u + d_2 \phi_z] dx$$

$$d_1 = 2\pi \left[P_i(x) \left(R - \frac{h}{2} \right) - P_o(x) \left(R + \frac{h}{2} \right) \right] \quad (18)$$

$$d_2 = 2\pi \frac{h}{2} \left[-P_i(x) \left(R - \frac{h}{2} \right) - P_o(x) \left(R + \frac{h}{2} \right) \right]$$

By considering the strain energy and external energy, functional of the system is defined as

$$U = \int_0^L (U_s - U_T) dx - \int_0^L W dx = \int_0^L F(u, w, \phi_x, \phi_z) dx \quad (19)$$

Euler equation for first order functional of four variables is presented as

$$\frac{\partial F}{\partial \chi_i} - \frac{\partial}{\partial x} \left(\frac{\partial F}{\partial \left(\frac{\partial \chi_i}{\partial x} \right)} \right) = 0, \quad \chi_i (i = 1, 2, 3, 4) = w, \phi_x, u, \phi_z \quad (20)$$

By substitution of functional in Euler relations, four differential equations of the system are derived as

$$\left\{ \begin{aligned} & 2(1-\nu)A_1 \frac{\partial^2 w}{\partial x^2} + 2(1-\nu)A_2 \frac{\partial^2 \phi_x}{\partial x^2} + 2\nu A_4 \frac{\partial u}{\partial x} + 2\nu(A_1 + A_6) \frac{\partial \phi_z}{\partial x} \\ & = \frac{\partial B_1(x)}{\partial x} + C_1 \left[(1-\nu) \frac{\partial \varepsilon_{xx}^c}{\partial x} + \nu \left(\frac{\partial \varepsilon_{rr}^c}{\partial x} + \frac{\partial \varepsilon_{\theta\theta}^c}{\partial x} \right) \right] \\ & 2(1-\nu)A_2 \frac{\partial^2 w}{\partial x^2} + 2(1-\nu)A_3 \frac{\partial^2 \phi_x}{\partial x^2} + [-K(1-2\nu)A_1 + 2\nu A_6] \frac{\partial u}{\partial x} \\ & + [-K(1-2\nu)A_2 + 2\nu(A_2 + A_9)] \frac{\partial \phi_z}{\partial x} - K(1-2\nu)A_1 \phi_x = \\ & \frac{\partial B_2(x)}{\partial x} - C_1 [K(1-2\nu)\varepsilon_{rx}^c] + C_2 \left[(1-\nu) \frac{\partial \varepsilon_{xx}^c}{\partial x} + \nu \left(\frac{\partial \varepsilon_{rr}^c}{\partial x} + \frac{\partial \varepsilon_{\theta\theta}^c}{\partial x} \right) \right] \\ & K(1-2\nu)A_1 \frac{\partial^2 u}{\partial x^2} + K(1-2\nu)A_2 \frac{\partial^2 \phi_x}{\partial x^2} - 2\nu A_4 \frac{\partial w}{\partial x} \\ & + [K(1-2\nu)A_1 - 2\nu A_6] \frac{\partial \phi_z}{\partial x} - 2(1-\nu)A_3 u \\ & - [2(1-\nu)A_7 + 2\nu A_4] \phi_z = -B_3(x) - d_1 \\ & -C_3 \left[(1-\nu)\varepsilon_{\theta\theta}^c + \nu(\varepsilon_{rr}^c + \varepsilon_{xx}^c) \right] + K(1-2\nu)C_1 \frac{\partial \varepsilon_{rx}^c}{\partial x} \\ & K(1-2\nu)A_2 \frac{\partial^2 u}{\partial x^2} + K(1-2\nu)A_3 \frac{\partial^2 \phi_x}{\partial x^2} - 2\nu(A_1 + A_6) \frac{\partial w}{\partial x} \\ & + [K(1-2\nu)A_2 - 2\nu(A_2 + A_9)] \frac{\partial \phi_z}{\partial x} - [2(1-\nu)A_7 + 2\nu A_4] u \\ & - [2(1-\nu)(A_1 + A_8) + 4\nu A_6] \phi_z = -B_1(x) - B_4(x) - d_2 \\ & -C_1 \left[(1-\nu)\varepsilon_{rr}^c + \nu(\varepsilon_{\theta\theta}^c + \varepsilon_{xx}^c) \right] \\ & -C_4 \left[(1-\nu)\varepsilon_{\theta\theta}^c + \nu(\varepsilon_{rr}^c + \varepsilon_{xx}^c) \right] + K(1-2\nu)C_2 \frac{\partial \varepsilon_{rx}^c}{\partial x} \end{aligned} \right. \quad (21)$$

In matrix form, Eq. (21) are presented as

$$\begin{cases} [G_1] \frac{d^2}{dx^2} \{X\} + [G_2] \frac{d}{dx} \{X\} + [G_3] \{X\} = \{F\} \\ \{X\} = \{w \quad \phi_x \quad u \quad \phi_z\}^T \end{cases} \quad (22)$$

In which, $\{G_i\}$ ($i = 1, 2, 3$), $\{F\}$ are presented in Appendix A.

4. Solution procedure; Elastic and creep solutions

4.1 General solution

The governing differential equations of the system are analytically solved to derive four unknown functions of the system. The solution procedure is containing homogeneous and particular solutions as follows

$$\{X\} = \{X\}_h + \{X\}_p \quad (23)$$

By considering the homogeneous solution as $\{X\}_h = \{v\}_i e^{m_i x}$, the homogeneous solution is obtained. In homogeneous solution, m_i are roots of eight's order characteristic equation and v_i are eigenvectors that defined as

$$[m^2 [G_1] + m [G_2] + [G_3]] = 0 \quad (24)$$

In general state, the homogeneous solution is defined as

$$\{X\}_h = \sum_{i=1}^6 c_i \{v\}_i e^{m_i x} + c_7 x + c_8 \quad (25)$$

The linear term arises from this fact that two zero roots are derived from characteristic equation.

4.2 Elastic solution

Particular solution of the differential equation for elastic is derived as

$$\{X\}_p = \{X\}_{p_1} + \{X\}_{p_2} \quad (26)$$

In which, $\{X\}_{p_1}$, $\{X\}_{p_2}$ are particular terms corresponding to thermal and mechanical loads, respectively. In this paper, we assume that pressure varies along the axial direction.

$$\left\{ \begin{aligned} w &= \sum_{n=1}^{\infty} A_n^w \sin(\zeta_n x) + \sum_{n=1}^{\infty} B_n^w \cos(\zeta_n x) + C^w x^2 + D^w x + E^w \\ \phi_x &= \sum_{n=1}^{\infty} A_n^{\phi_x} \sin(\zeta_n x) + \sum_{n=1}^{\infty} B_n^{\phi_x} \cos(\zeta_n x) + C^{\phi_x} x^2 + D^{\phi_x} x + E^{\phi_x} \\ u &= \sum_{n=1}^{\infty} A_n^u \sin(\zeta_n x) + \sum_{n=1}^{\infty} B_n^u \cos(\zeta_n x) + C^u x^2 + D^u x + E^u \\ \phi_z &= \sum_{n=1}^{\infty} A_n^{\phi_z} \sin(\zeta_n x) + \sum_{n=1}^{\infty} B_n^{\phi_z} \cos(\zeta_n x) + C^{\phi_z} x^2 + D^{\phi_z} x + E^{\phi_z} \end{aligned} \right. \quad (27)$$

One can find that the first two terms arises from thermal

loads and temperature distribution and second three terms arises from axial variable pressure distribution. Substitution of obtained particular solution in differential equations of the system (Eq. (22)) yields

$$\begin{aligned}
 & -\zeta_n^2 [G_1] (\{A_n\} \sin(\zeta_n x) + \{B_n\} \cos(\zeta_n x)) \\
 & + \zeta_n [G_2] (\{A_n\} \cos(\zeta_n x) - \{B_n\} \sin(\zeta_n x)) \\
 & + [G_3] (\{A_n\} \sin(\zeta_n x) + \{B_n\} \cos(\zeta_n x)) \\
 & = \left\{ \begin{array}{c} \frac{\partial B_1(x)}{\partial x} \\ \frac{\partial B_2(x)}{\partial x} \\ -B_3(x) \\ -(B_1(x) + B_4(x)) \end{array} \right\} \quad (28)
 \end{aligned}$$

Arranging the similar terms yields two distinct relations as

$$\begin{aligned}
 & -\zeta_n^2 [G_1] \{A_n\} \sin(\zeta_n x) - \zeta_n [G_2] \{B_n\} \sin(\zeta_n x) \\
 & + [G_3] \{A_n\} \sin(\zeta_n x) = \left\{ \begin{array}{c} 0 \\ 0 \\ -B_3(x) \\ -(B_1(x) + B_4(x)) \end{array} \right\} \\
 & -\zeta_n^2 [G_1] \{B_n\} \cos(\zeta_n x) + \zeta_n [G_2] \{A_n\} \cos(\zeta_n x) \quad (29) \\
 & + [G_3] \{B_n\} \cos(\zeta_n x) = \left\{ \begin{array}{c} \frac{\partial B_1(x)}{\partial x} \\ \frac{\partial B_2(x)}{\partial x} \\ 0 \\ 0 \end{array} \right\}
 \end{aligned}$$

Second particular solutions $\{X\}_{p_2}$ are corresponding to inner and outer axially variable pressures which are assumed in general case, second order along the longitudinal direction as

$$\begin{cases} P_i(x) = A_i x^2 + B_i x + C_i \\ P_o(x) = A_o x^2 + B_o x + C_o \end{cases} \quad (30)$$

Based on the mentioned descriptions, particular solutions are expressed as

$$\begin{aligned}
 \{X\}_{p_2} &= \begin{Bmatrix} C^w \\ C^{\phi_x} \\ C^u \\ C^{\phi_z} \end{Bmatrix} x^2 + \begin{Bmatrix} D^w \\ D^{\phi_x} \\ D^u \\ D^{\phi_z} \end{Bmatrix} x + \begin{Bmatrix} E^w \\ E^{\phi_x} \\ E^u \\ E^{\phi_z} \end{Bmatrix} \quad (31) \\
 \rightarrow \{X\}_{p_2} &= \{C\} x^2 + \{D\} x + \{E\}
 \end{aligned}$$

Substitution of above particular solution in differential equations of the system yields three unknown matrices $\{C\}$, $\{D\}$, $\{E\}$ in Eq. (30) as follows

$$\begin{cases} \{C\} = [G_3]^{-1} \{F_2\} \\ \{D\} = [G_3]^{-1} (\{F_1\} - 2[G_2]\{C\}) \\ \{E\} = [G_3]^{-1} (\{F_0\} - 2[G_1]\{C\} - [G_2]\{D\}) \end{cases} \quad (32)$$

At the end general and particular solutions for elastic case are presented as

$$\{X\} = \sum_{i=1}^6 c_i \{v\}_i e^{m_i x} + c_7 x + c_8 + \{X\}_p \quad (33)$$

4.2 Creep solution

Creep strain rates in radial, tangential and axial directions are related to the current stresses and the material creep constitutive model by the Prandtl-Reuss equations (Penny and Marriott 1971, Kraus 1980) as

$$\begin{aligned}
 \dot{\epsilon}_{rr}^c &= \frac{\dot{\epsilon}_e}{\sigma_e} \left[\sigma_{rr} - \frac{1}{2} (\sigma_{\theta\theta} + \sigma_{xx}) \right] \\
 \dot{\epsilon}_{\theta\theta}^c &= \frac{\dot{\epsilon}_e}{\sigma_e} \left[\sigma_{\theta\theta} - \frac{1}{2} (\sigma_{rr} + \sigma_{xx}) \right] \\
 \dot{\epsilon}_{xx}^c &= \frac{\dot{\epsilon}_e}{\sigma_e} \left[\sigma_{xx} - \frac{1}{2} (\sigma_{rr} + \sigma_{\theta\theta}) \right] \\
 \dot{\epsilon}_{rx}^c &= \frac{3}{2} \frac{\dot{\epsilon}_e}{\sigma_e} \tau_{rx} \quad (34)
 \end{aligned}$$

The uniaxial creep constitutive model is the Norton's law that is defined as

$$\dot{\epsilon}_e^c = B(r) \sigma_e^{n(r)} \quad (35)$$

where r is the radial coordinate and $B(r)$ and $n(r)$ are the radial-dependent material creep parameters. In this study $B(r) = b_0 r^{b_1}$ and $n(r)$ is considered to be a constant $n(r) = n_0$. Substituting Eq. (35) into Eqs. (34), the relationships between radial and tangential strain rates and radial and tangential stresses become

$$\begin{aligned}
 \dot{\epsilon}_{rr}^c &= b_0 r^{b_1} \sigma_e^{n_0-1} \left[\sigma_{rr} - \frac{1}{2} (\sigma_{\theta\theta} + \sigma_{xx}) \right] \\
 \dot{\epsilon}_{\theta\theta}^c &= b_0 r^{b_1} \sigma_e^{n_0-1} \left[\sigma_{\theta\theta} - \frac{1}{2} (\sigma_{rr} + \sigma_{xx}) \right] \\
 \dot{\epsilon}_{xx}^c &= b_0 r^{b_1} \sigma_e^{n_0-1} \left[\sigma_{xx} - \frac{1}{2} (\sigma_{rr} + \sigma_{\theta\theta}) \right] \\
 \dot{\epsilon}_{rx}^c &= \frac{3}{2} b_0 r^{b_1} \sigma_e^{n_0-1} \tau_{rx} \quad (36)
 \end{aligned}$$

Here, the Von-mises effective stress σ_e is written as

$$\sigma_e = \frac{1}{\sqrt{2}} \left[(\sigma_{rr} - \sigma_{\theta\theta})^2 + (\sigma_{rr} - \sigma_{xx})^2 + (\sigma_{\theta\theta} - \sigma_{xx})^2 + 6\tau_{rx}^2 \right]^{1/2} \quad (37)$$

Considering the pressure and temperature fields to be

steady, the four differential equation of the system (Eq. (21)) containing creep strains may be rewritten in terms of creep strain rates of follows

$$\begin{cases}
 2(1-\nu)A_1 \frac{\partial^2 \dot{w}}{\partial x^2} + 2(1-\nu)A_2 \frac{\partial^2 \dot{\phi}_x}{\partial x^2} + 2\nu A_4 \frac{\partial \dot{u}}{\partial x} + 2\nu(A_1 + A_6) \frac{\partial \dot{\phi}_z}{\partial x} \\
 = C_1 [(1-\nu) \frac{\partial \dot{\epsilon}_{xx}^c}{\partial x} + \nu \left(\frac{\partial \dot{\epsilon}_{rr}^c}{\partial x} + \frac{\partial \dot{\epsilon}_{\theta\theta}^c}{\partial x} \right)] \\
 2(1-\nu)A_2 \frac{\partial^2 \dot{w}}{\partial x^2} + 2(1-\nu)A_3 \frac{\partial^2 \dot{\phi}_x}{\partial x^2} + [-K(1-2\nu)A_1 + 2\nu A_6] \frac{\partial \dot{u}}{\partial x} \\
 + [-K(1-2\nu)A_2 + 2\nu(A_2 + A_9)] \frac{\partial \dot{\phi}_z}{\partial x} - K(1-2\nu)A_1 \dot{\phi}_z \\
 = -KC_1 [(1-2\nu) \dot{\epsilon}_{xx}^c] + C_2 \left[(1-\nu) \frac{\partial \dot{\epsilon}_{xx}^c}{\partial x} + \nu \left(\frac{\partial \dot{\epsilon}_{rr}^c}{\partial x} + \frac{\partial \dot{\epsilon}_{\theta\theta}^c}{\partial x} \right) \right] \\
 K(1-2\nu)A_1 \frac{\partial^2 \dot{u}}{\partial x^2} + K(1-2\nu)A_2 \frac{\partial^2 \dot{\phi}_z}{\partial x^2} - 2\nu A_4 \frac{\partial \dot{w}}{\partial x} + \\
 [K(1-2\nu)A_1 - 2\nu A_6] \frac{\partial \dot{\phi}_z}{\partial x} - 2(1-\nu)A_3 \dot{u} - [2(1-\nu)A_7 + 2\nu A_4] \dot{\phi}_z \\
 = K(1-2\nu)C_1 \frac{\partial \dot{\epsilon}_{rr}^c}{\partial x} - C_3 \left[(1-\nu) \dot{\epsilon}_{\theta\theta}^c + \nu (\dot{\epsilon}_{rr}^c + \dot{\epsilon}_{xx}^c) \right] \\
 K(1-2\nu)A_2 \frac{\partial^2 \dot{u}}{\partial x^2} + K(1-2\nu)A_3 \frac{\partial^2 \dot{\phi}_z}{\partial x^2} - 2\nu(A_1 + A_6) \frac{\partial \dot{w}}{\partial x} \\
 + [K(1-2\nu)A_2 - 2\nu(A_2 + A_9)] \frac{\partial \dot{\phi}_z}{\partial x} - [2(1-\nu)A_7 + 2\nu A_4] \dot{u} \\
 - [2(1-\nu)(A_1 + A_8) + 4\nu A_6] \dot{\phi}_z = K(1-2\nu)C_2 \frac{\partial \dot{\epsilon}_{rr}^c}{\partial x} \\
 - C_1 \left[(1-\nu) \dot{\epsilon}_{rr}^c + \nu (\dot{\epsilon}_{\theta\theta}^c + \dot{\epsilon}_{xx}^c) \right] - C_4 \left[(1-\nu) \dot{\epsilon}_{\theta\theta}^c + \nu (\dot{\epsilon}_{rr}^c + \dot{\epsilon}_{xx}^c) \right]
 \end{cases} \quad (38)$$

Substituting Eqs. (36) into Eqs. (38), and Consider $\mu_1 = \frac{b_0 r^{b_1}}{2}(1-2\nu)$ the final form of four differential equation of the system (Eq. (38)) become

$$\begin{cases}
 2(1-\nu)A_1 \frac{\partial^2 \dot{w}}{\partial x^2} + 2(1-\nu)A_2 \frac{\partial^2 \dot{\phi}_x}{\partial x^2} + 2\nu A_4 \frac{\partial \dot{u}}{\partial x} + 2\nu(A_1 + A_6) \frac{\partial \dot{\phi}_z}{\partial x} \\
 = \mu_1 C_1 (n_0 - 1) \sigma_e^{n_0-2} \frac{\partial \sigma_e}{\partial x} \times [2\sigma_{xx} - (\sigma_{rr} + \sigma_{\theta\theta})] \\
 + \mu_1 C_1 \sigma_e^{n_0-1} \left[2 \frac{\partial \sigma_{xx}}{\partial x} - \left(\frac{\partial \sigma_{rr}}{\partial x} + \frac{\partial \sigma_{\theta\theta}}{\partial x} \right) \right] \\
 2(1-\nu)A_2 \frac{\partial^2 \dot{w}}{\partial x^2} + 2(1-\nu)A_3 \frac{\partial^2 \dot{\phi}_x}{\partial x^2} + [-K(1-2\nu)A_1 + 2\nu A_6] \frac{\partial \dot{u}}{\partial x} \\
 + [-K(1-2\nu)A_2 + 2\nu(A_2 + A_9)] \frac{\partial \dot{\phi}_z}{\partial x} - K(1-2\nu)A_1 \dot{\phi}_z \\
 = -3K \mu_1 C_1 \sigma_e^{n_0-1} \tau_{rx} + \mu_1 C_2 (n_0 - 1) \sigma_e^{n_0-2} \frac{\partial \sigma_e}{\partial x} [2\sigma_{xx} - (\sigma_{rr} + \sigma_{\theta\theta})] \\
 + \mu_1 C_2 \sigma_e^{n_0-1} \left[2 \frac{\partial \sigma_{xx}}{\partial x} - \left(\frac{\partial \sigma_{rr}}{\partial x} + \frac{\partial \sigma_{\theta\theta}}{\partial x} \right) \right] \\
 K(1-2\nu)A_1 \frac{\partial^2 \dot{u}}{\partial x^2} + K(1-2\nu)A_2 \frac{\partial^2 \dot{\phi}_z}{\partial x^2} - 2\nu A_4 \frac{\partial \dot{w}}{\partial x} + \\
 [K(1-2\nu)A_1 - 2\nu A_6] \frac{\partial \dot{\phi}_z}{\partial x} - 2(1-\nu)A_3 \dot{u} - [2(1-\nu)A_7 + 2\nu A_4] \dot{\phi}_z \\
 = 3K \mu_1 C_1 \left[(n_0 - 1) \sigma_e^{n_0-2} \frac{\partial \sigma_e}{\partial x} \tau_{rx} + \sigma_e^{n_0-1} \frac{\partial \tau_{rx}}{\partial x} \right] \\
 + \mu_1 C_3 \sigma_e^{n_0-1} [2\sigma_{\theta\theta} - (\sigma_{rr} + \sigma_{xx})] \\
 K(1-2\nu)A_2 \frac{\partial^2 \dot{u}}{\partial x^2} + K(1-2\nu)A_3 \frac{\partial^2 \dot{\phi}_z}{\partial x^2} - 2\nu(A_1 + A_6) \frac{\partial \dot{w}}{\partial x} \\
 + [K(1-2\nu)A_2 - 2\nu(A_2 + A_9)] \frac{\partial \dot{\phi}_z}{\partial x} - [2(1-\nu)A_7 + 2\nu A_4] \dot{u} \\
 - [2(1-\nu)(A_1 + A_8) + 4\nu A_6] \dot{\phi}_z = +3K \mu_1 C_2 [(n_0 - 1) \sigma_e^{n_0-2} \frac{\partial \sigma_e}{\partial x} \tau_{rx} \\
 + \sigma_e^{n_0-1} \frac{\partial \tau_{rx}}{\partial x}] - \mu_1 \left[C_1 [2\sigma_{rr} - (\sigma_{\theta\theta} + \sigma_{xx})] + C_4 [2\sigma_{\theta\theta} - (\sigma_{rr} + \sigma_{xx})] \right]
 \end{cases} \quad (39)$$

in matrix form, Eq. (39) are expressed as

$$\begin{cases}
 [G_1] \frac{d^2}{dx^2} \{y\} + [G_2] \frac{d}{dx} \{y\} + [G_3] \{y\} = \{F_c\} \\
 \{\dot{X}\} = \{w \quad \dot{\phi}_x \quad u \quad \dot{\phi}_z\}^T
 \end{cases} \quad (40)$$

In which, $\{F_c\}$ are presented in Appendix A. The procedure of general solution is same as procedure in part 5.1 as

$$\{\dot{X}\}_n = \sum_{i=1}^6 \dot{c}_i \{v\}_i e^{m_i x} + \dot{c}_7 x + \dot{c}_8 \quad (41)$$

Given that $\{F_c\}$ is comprised of constant parameters, for the particular part of solution of Eqs. (38), the particular solution can be expressed as follows

$$[G_3] \{\dot{X}\}_p = \{F_c\} \rightarrow \{\dot{X}\}_p = [G_3]^{-1} \{F_c\} \quad (42)$$

Finally, the total solution of creep is a summation of the general and the particular solution.

$$\{\dot{X}\} = \sum_{i=1}^6 \dot{c}_i \{v\}_i e^{m_i x} + \dot{c}_7 x + \dot{c}_8 + \{\dot{X}\}_p \quad (43)$$

After derivation of homogeneous and particular solutions for elastic or creep state, the boundary conditions may be applied on the total solution. In this paper, we consider a clamped-clamped short cylindrical shell. For this type of boundary conditions, it is defined as

$$x = 0, L \rightarrow \begin{cases} w = 0 \\ \dot{\phi}_x = 0 \\ u = 0 \\ \dot{\phi}_z = 0 \end{cases} \quad (44)$$

5. Numerical result

In this section, numerical results of present formulation are shown. The numerical results are including elastic and creep solutions. The longitudinally variable pressure is assumed as Fig. 2. And Inner and outer temperature loading

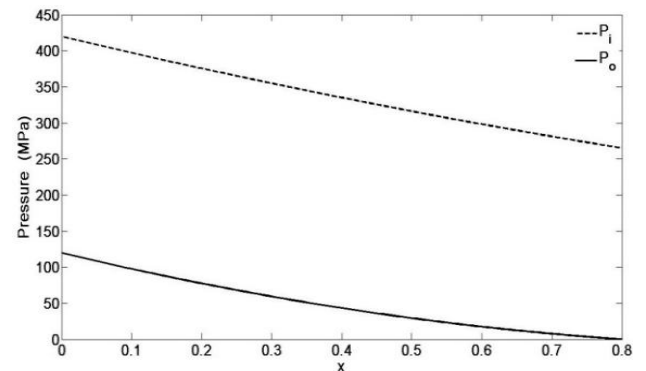


Fig. 2 Longitudinally variable pressure in terms of length of the cylinder

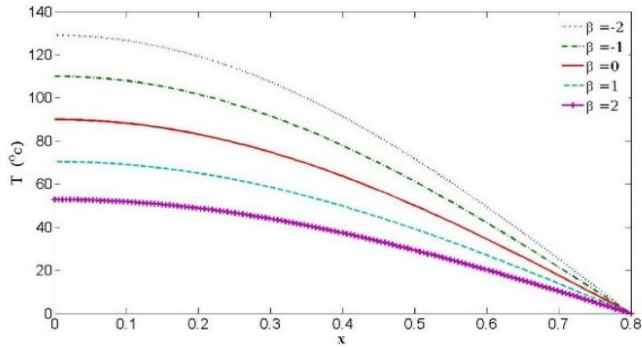


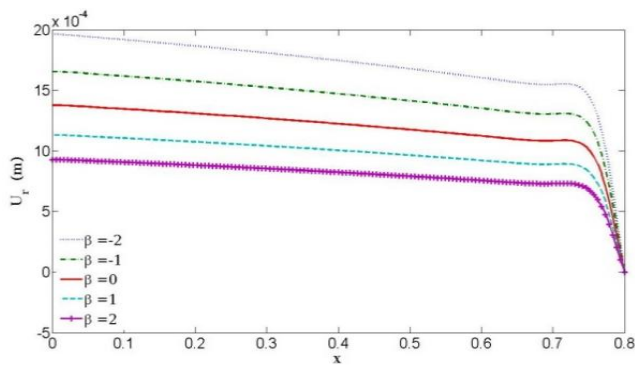
Fig. 3 The axial distribution of temperature for different values of non-homogeneous index

along the axial direction is considered as $T_i = 200 \sin\left(\frac{n\pi x}{L}\right)$ and $T_o = 0$, respectively. The obtained results are classified as elastic and creep results.

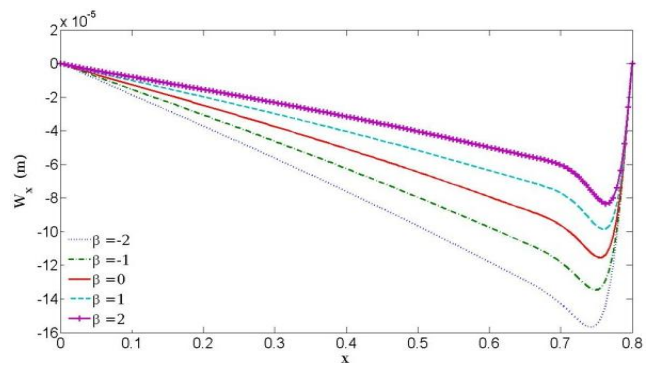
5.1 Elastic

In this section, both thermal and mechanical loadings are applied on the cylinder. Shown in Fig. 3 is the axial distribution of temperature for different values of non-homogeneous index. The obtained results indicate that with increasing the non-homogeneous index, the temperature is decreased significantly.

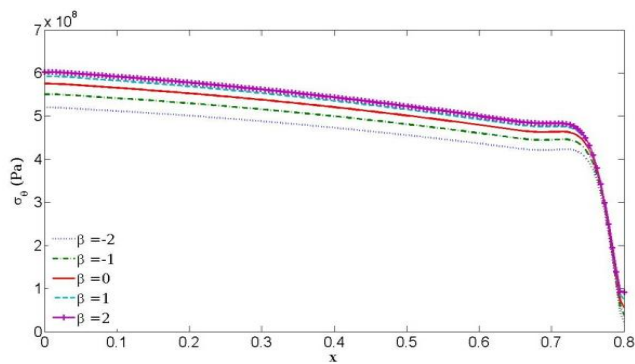
Shown in Figs. 4(a), (b), (c) and (d) is the axial distribu-



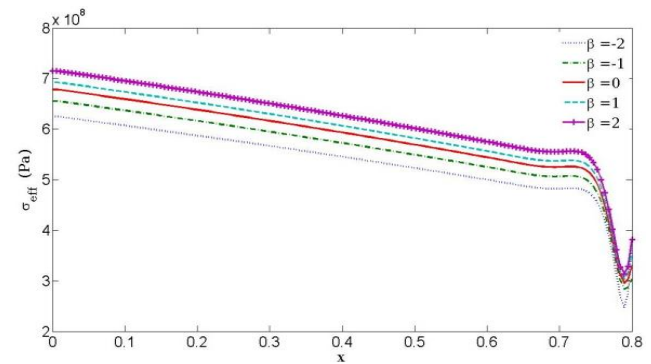
(a) Radial displacement



(b) Axial displacement

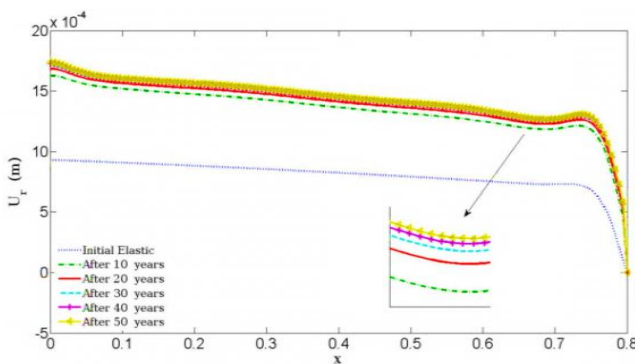


(c) Circumferential stress

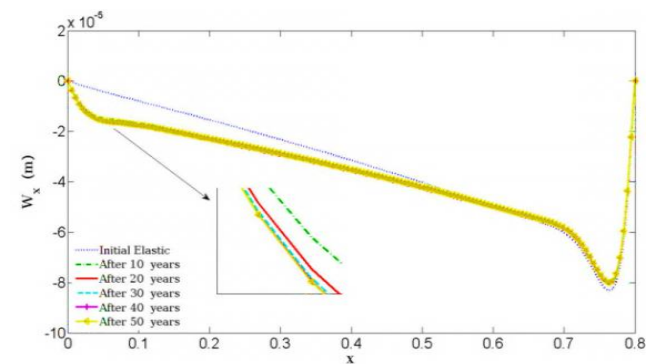


(d) Effective stress

Fig. 4 The radial distribution of radial and axial displacements, circumferential and effective stresses



(a) Radial displacement



(d) Effective stress

Fig. 5 The History of radial distribution of radial and axial displacements for 10, 20, 30, 40 and 50 years

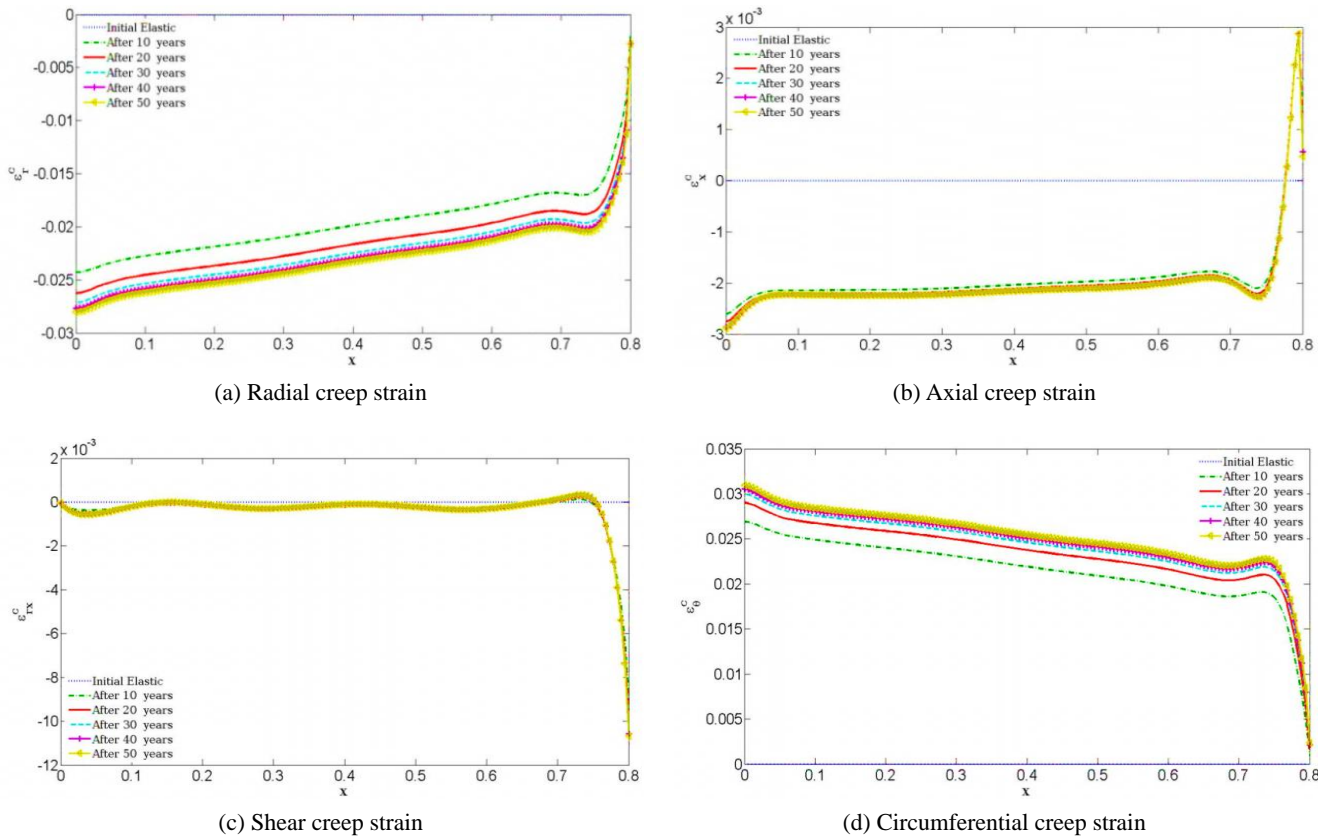


Fig. 6 The History of radial distribution of radial, axial, shear and circumferential creep strains for 10, 20, 30, 40 and 50 years

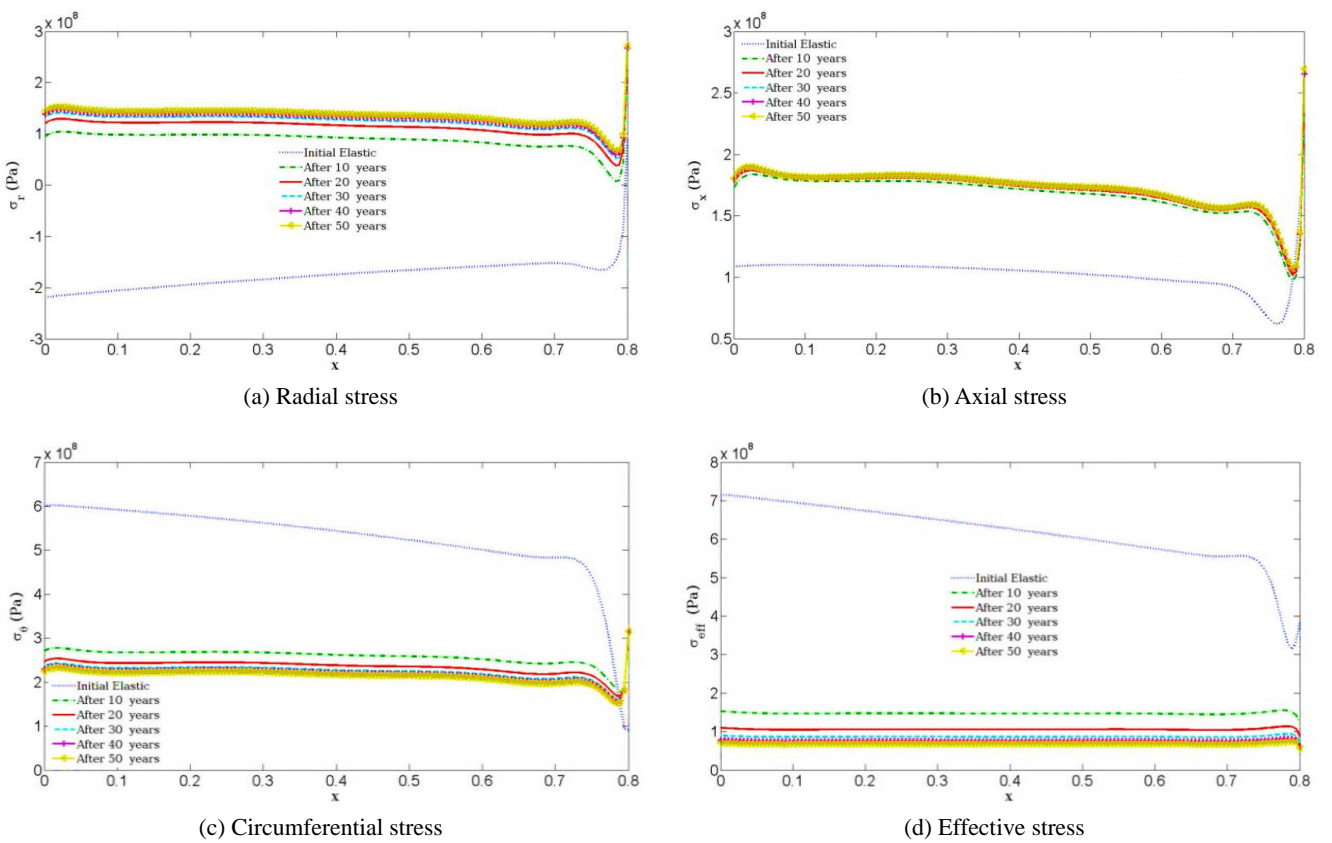


Fig. 7 The History of radial distribution of radial, axial, circumferential and effective stresses for 10, 20, 30, 40 and 50 years

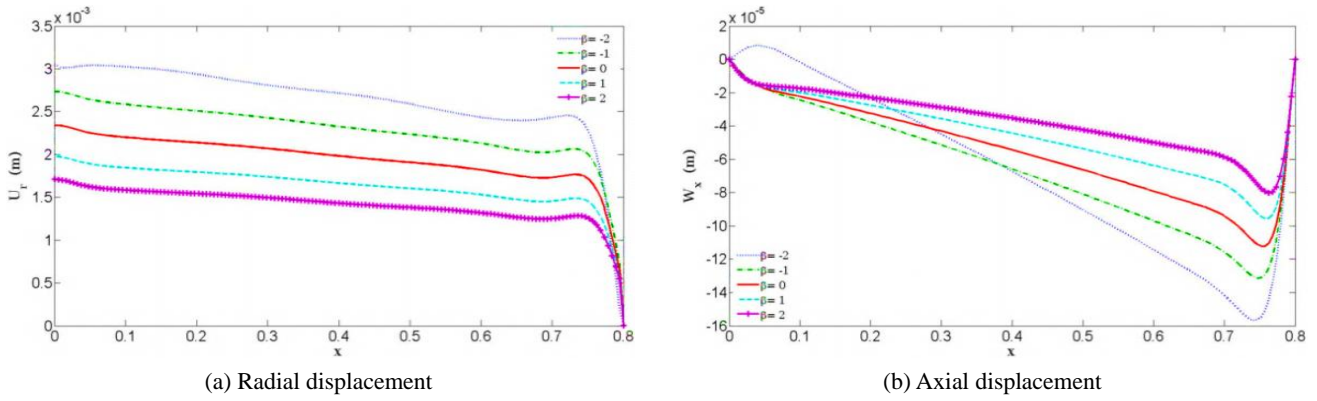


Fig. 8 The history of radial distribution of radial and axial displacements after 30 years for $\beta = 2$

tion of radial and axial displacements, circumferential and effective stresses in terms of different values of non-homogeneous index of used material.

5.2 Creep

In this section, the histories of thermo-elastic results for 50 years are presented. Shown in Fig. 5 is longitudinal distribution of axial and radial displacements for different interval of creep time. It can be concluded with increasing the creep time, the different curves leads to a uniform condition.

Fig. 6 shows history of creep strains (longitudinal, circumferential, radial and shear strains) along the longitudinal direction for different creep times. The

obtained results show that with increasing the creep time, all strain curves tend to a uniform variation. Furthermore, it can be concluded that the boundaries of cylinder have significant effects on the creep strains.

Shown in Fig. 7 are histories of creep stress (longitudinal, circumferential, radial and shear strains) along the longitudinal direction for different creep times. The obtained results show that with increasing the creep time, all stress curves tend to a uniform variation. Furthermore, it can be concluded that the boundaries of cylinder have significant effects on the creep strains. The main conclusion of this figure is significant reduction of circumferential stress for greater times of creep. This reduction leads to important decreasing the effective stress.

In this section, the influence of non-homogeneous index

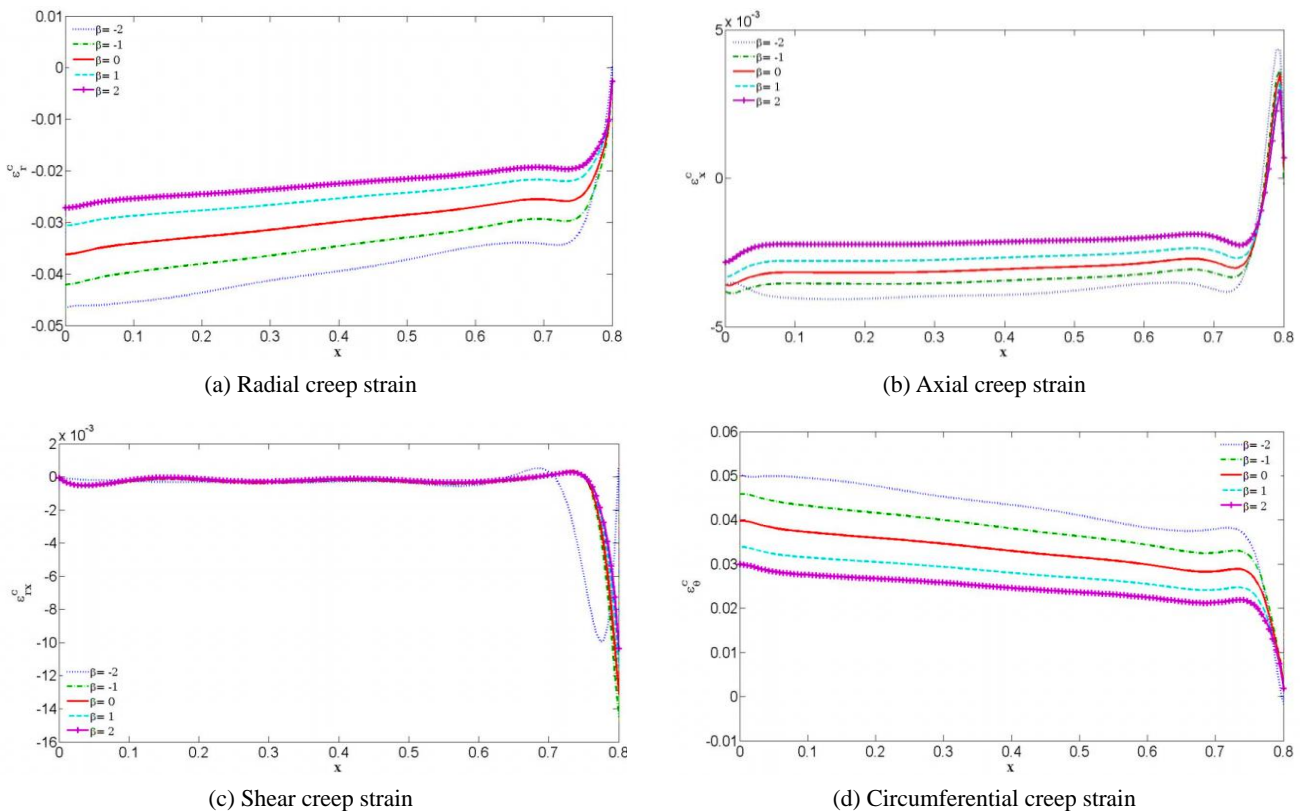


Fig. 9 The History of radial distribution of radial, axial, shear and circumferential creep strains after 30 years for $\beta = 2$

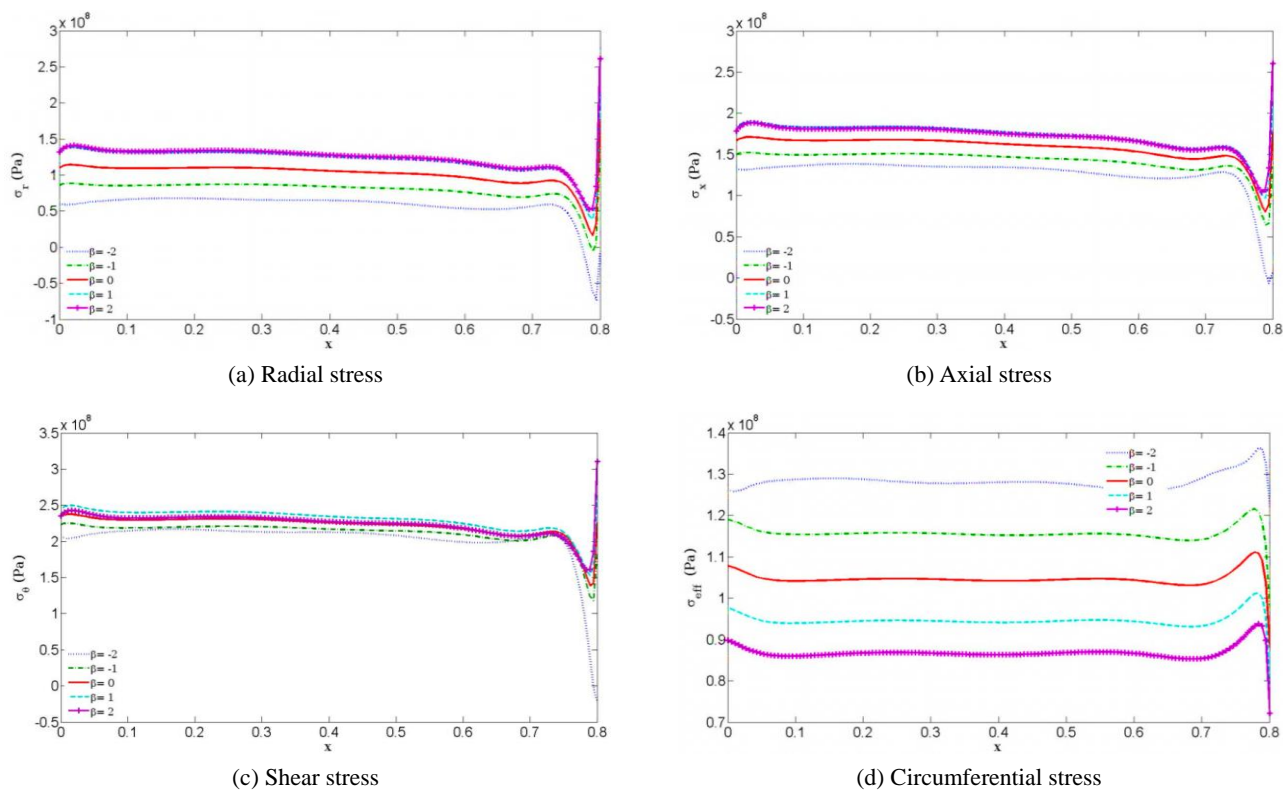


Fig. 10 The History of radial distribution of radial, axial, circumferential and effective stress after 30 years for $\beta = 2$

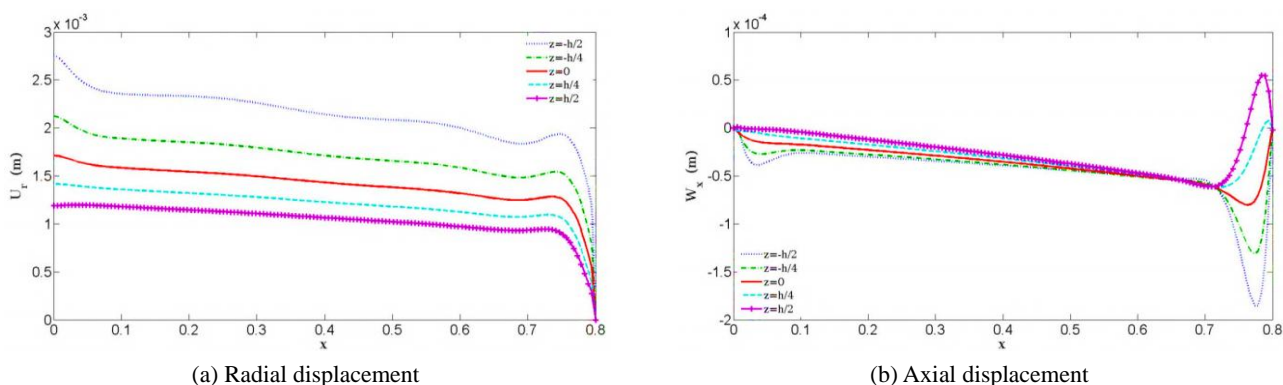


Fig. 11 The longitudinal distribution of radial and axial displacements after 30 years for $\beta = 2$ and $z = -h / 2, -h / 4, 0, h / 4, h / 4$

on the different responses of cylinder is investigated. The distribution of axial and radial displacements after 30 years along the axial direction is presented for different values of non-homogeneous index in Fig. 8.

The influence of non homogeneous index on the distribution of different strains (longitudinal, circumferential, radial and shear strains) along the longitudinal direction after 30 years is presented in Fig. 9.

The influence of non homogeneous index on the distribution of different stress components (longitudinal, circumferential, radial and shear stresses) along the longitudinal direction after 30 years is presented in Fig. 10.

As final results, the numerical values of displacements and stress for different layers of cylinder are presented. Fig. 11 shows the longitudinal variation of radial and

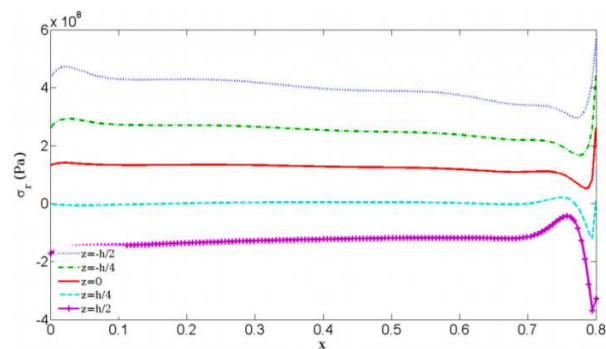


Fig. 12 The History of radial distribution of radial stress after 30 years for $\beta = 2$ and $z = -h / 2, -h / 4, 0, h / 4, h / 4$

longitudinal displacements of cylinder for different radial locations ($z = -h/2, -h/4, 0, h/4, h/4$) after 30 years.

Shown in Fig. 12 is longitudinal distribution of radial for different radial locations ($z = -h/2, -h/4, 0, h/4, h/4$) after 30 years. The influence of boundaries on the results of cylinder can be observed in this figure.

6. Conclusions

Two dimensional time dependent creep analysis of a functionally graded hollow cylinder subjected to longitudinally variable thermal and mechanical loads was studied in this paper using first order shear deformation theory and Yang method. The history of stress, strains and deformations was derived for different values of non homogeneous index and after various time intervals. The numerical results indicate that the boundaries of cylinder and non homogeneous index can significantly change the creep behavior of functionally graded cylindrical shell. Furthermore, the effect of creep time on the behavior of cylinder for various values of non homogeneous index leads to interesting results and conclusions for engineers and designers. Some important results of this paper is presented as:

- (1) The numerical results indicate that with increasing the non homogeneous index, the radial and longitudinal deformations are increased while the stress components are decreased.
- (2) Investigation on the creep time indicates that with increasing the creep time, the different curves leads to a uniform condition.

References

- Abdelbaki, C., Tounsi, A., Habib, H. and Hassan, S. (2017), "Thermal buckling analysis of cross-ply laminated plates using a simplified HSDT", *Smart Struct. Syst., Int. J.*, **19**(3), 289-297.
- Arefi, M. (2014), "A complete set of equations for piezo-magnetoelastic analysis of a functionally graded thick shell of revolution", *Latin Am. J. Solids. Struct.*, **11**(11), 2073-2092.
- Arefi, M. and Bidgoli, E.M.R. (2017), "Elastic solution of a constrained FG short cylinder under axially variable pressure", *J. Inst. Eng. (Ind): Series C.*, **98**(3), 267-276.
- Arefi, M. and Khoshgoftar, M.J. (2014), "Comprehensive piezo-thermo-elastic analysis of a thick hollow spherical shell", *Smart. Struct. Syst., Int. J.*, **14**(2), 225-246.
- Arefi, M. and Rahimi, G.H. (2010), "Thermo elastic analysis of a functionally graded cylinder under internal pressure using first order shear deformation theory", *Sci. Res. Essays.*, **5**(12), 1442-1454.
- Arefi, M. and Rahimi, G.H. (2011), "Non linear analysis of a functionally graded square plate with two smart layers as sensor and actuator under normal pressure", *Smart. Struct. Syst., Int. J.*, **8**(5), 433-447.
- Arefi, M. and Rahimi, G.H. (2012a), "The effect of nonhomogeneity and end supports on the thermo elastic behavior of a clamped-clamped FG cylinder under mechanical and thermal loads", *Int. J. Press. Ves. Pip.*, **96**, 30-37.
- Arefi, M. and Rahimi, G.H. (2012b), "Comprehensive thermoelastic analysis of a functionally graded cylinder with different boundary conditions under internal pressure using first order shear deformation theory", *Mechanika.*, **18**(1), 5-13.
- Arefi, M. and Rahimi, G.H. (2012c), "Studying the nonlinear behavior of the functionally graded annular plates with piezoelectric layers as a sensor and actuator under normal pressure", *Smart. Struct. Syst., Int. J.*, **9**(2), 127-143.
- Arefi, M. and Rahimi, G.H. (2014), "Application of shear deformation theory for two dimensional electro-elastic analysis of a FGP cylinder", *Smart. Struct. Syst., Int. J.*, **14**(2), 225-246.
- Arefi, M. and Zenkour, A.M. (2016), "Employing sinusoidal shear deformation plate theory for transient analysis of three layers sandwich nanoplate integrated with piezo-magnetic face-sheets", *Smart Mater. Struct.*, **25**(11), 115040.
- Arefi, M. and Zenkour, A.M. (2017a), "Nonlocal electro-thermo-mechanical analysis of a sandwich nanoplate containing a Kelvin-Voigt viscoelastic nanoplate and two piezoelectric layers", *Acta. Mech.*, **228**(2), 475-493.
- Arefi, M. and Zenkour, A.M. (2017b), "Thermo-electro-mechanical bending behavior of sandwich nanoplate integrated with piezoelectric face-sheets based on trigonometric plate theory", *Compos. Struct.*, **162**, 108-122.
- Arefi, M., Rahimi, G.H. and Khoshgoftar, M.J. (2011), "Optimized design of a cylinder under mechanical, magnetic and thermal loads as a sensor or actuator using a functionally graded piezomagnetic material", *Int. J. Phys. Sci.*, **6**(27), 6315-6322.
- Arefi, M., Rahimi, G.H. and Khoshgoftar, M.J. (2012), "Exact solution of a thick walled functionally graded piezoelectric cylinder under mechanical, thermal and electrical loads in the magnetic field", *Smart Struct. Syst., Int. J.*, **9**(5), 427-439.
- Arefi, M., Abbasi A.R. and Vaziri Sereshk, M.R. (2016a), "Two-dimensional thermoelastic analysis of FG cylindrical shell resting on the Pasternak foundation subjected to mechanical and thermal loads based on FSDT formulation", *J. Therm. Stresses.*, **39**(5), 554-570.
- Arefi, M., Faegh, R.K. and Loghman, A. (2016b), "The effect of axially variable thermal and mechanical loads on the 2D thermoelastic response of FG cylindrical shell", *J. Therm. Stress.*, **39**(12), 1539-1559.
- Arefi, M., Karroubi, R. and Irani-Rahaghi M. (2016c), "Free vibration analysis of functionally graded laminated sandwich cylindrical shells integrated with piezoelectric layer", *Appl. Math. Mech. (Engl Ed.)*, **37**(7), 821-834.
- Beldjelili, Y., Tounsi, A. and Hassan, S. (2016), "Hygro-thermo-mechanical bending of S-FGM plates resting on variable elastic foundations using a four-variable trigonometric plate theory", *Smart Struct. Syst., Int. J.*, **18**(4), 755-786.
- Bellifa, H., Benrahou, K.H., Hadji, L., Houari, M.S.A. and Tounsi, A. (2016), "Bending and free vibration analysis

- of functionally graded plates using a simple shear deformation theory and the concept the neutral surface position”, *J. Braz. Soc. Mech. Sci. Eng.*, **38**(1), 265-275.
- Bouderba, B., Tounsi, A. and Houari, M.S.A. (2013), “Thermomechanical bending response of FGM thick plates resting on Winkler–Pasternak elastic foundations”, *Steel Compos. Struct., Int. J.*, **14**(1), 85-104.
- Bouderba, B., Houari, M.S.A., Tounsi, A. and Mahmoud, S.R. (2016), “Thermal stability of functionally graded sandwich plates using a simple shear deformation theory”, *Struct. Eng. Mech., Int. J.*, **58**(3), 397-422.
- Bounouara, F., Benrahou, K.H., Belkorissat, I. and Tounsi, A. (2016), “A nonlocal zeroth-order shear deformation theory for free vibration of functionally graded nanoscale plates resting on elastic foundation”, *Steel Compos. Struct., Int. J.*, **20**(2), 227-249.
- Bourada, M., Kaci, A., Houari, M.S.A. and Tounsi, A. (2015), “A new simple shear and normal deformations theory for functionally graded beams”, *Steel Compos. Struct., Int. J.*, **18**(2), 409-423.
- Bousahla, A.A., Benyoucef, S., Tounsi, A. and Mahmoud, S.R. (2016), “On thermal stability of plates with functionally graded coefficient of thermal expansion”, *Struct. Eng. Mech., Int. J.*, **60**(2), 313-335.
- Brcic, J., Canadija, M., Turkalj, G., Krscanski, S., Lanc, D., Brcic, M. and Gao, Z. (2016), “Short-time creep, fatigue and mechanical properties of 42CrMo4 - Low alloy structural steel”, *Steel Compos. Struct., Int. J.*, **22**(4), 875-888.
- Dai, H.L. and Fu, Y.M. (2007), “Magnetothermoelastic interactions in hollow structures of functionally graded material subjected to mechanical load”, *Int. J. Press. Ves. Pip.*, **84**(3), 132-138.
- Draiche, K., Tounsi, A. and Hassan, S. (2016), “A refined theory with stretching effect for the flexure analysis of laminated composite plates”, *Geomech. Eng., Int. J.*, **11**(5), 671-690.
- El-Haina, F., Bakora, A., Bousahla, A.A., Tounsi, A. and Mahmoud, S.R. (2017), “A simple analytical approach for thermal buckling of thick functionally graded sandwich plates”, *Struct. Eng. Mech., Int. J.*, **63**(5), 585-595.
- Hamidi, A., Houari, M.S.A., Mahmoud, S.R. and Tounsi, A. (2015), “A sinusoidal plate theory with 5-unknowns and stretching effect for thermomechanical bending of functionally graded sandwich plates”, *Steel Compos. Struct., Int. J.*, **18**(1), 235-253.
- Jabbari, M., Sohrabpour, S. and Eslami, M.R. (2002), “Mechanical and thermal stresses in a functionally graded hollow cylinder due to radially symmetric loads”, *Int. J. Press. Vessels. Pip.*, **79**(7), 493-497.
- Jabbari, M. and Bahtui, A. and Eslami, M.R. (2009), “Axisymmetric mechanical and thermal stresses in thick short length FGM cylinders”, *Int. J. Press. Vessels. Pip.*, **86**(5), 296-306.
- Kelesm, I. and Conker, C. (2011), “Transient hyperbolic heat conduction in thick-walled FGM cylinders and spheres with exponentially-varying properties”, *Eur. J. Mech. A/Solids*, **30**(3), 449-455.
- Keles, I. and Tutuncu, N. (2011), “Exact analysis of axisymmetric dynamic response of functionally graded cylinders (or disks) and spheres”, *J. Appl. Mech.*, **78**(6), 610-614.
- Kheirkhah, S. and Loghman, A. (2015), “Electric potential redistribution due to time-dependent creep in thick-walled FGPM cylinder based on Mendelson method of successive approximation”, *Struct. Eng. Mech., Int. J.*, **53**(6), 1167-1182.
- Khoshgoftar, M.J., Rahimi, G.H. and Arefi, M. (2013), “Exact solution of functionally graded thick cylinder with finite length under longitudinally non-uniform pressure”, *Mech. Res. Com.*, **51**, 61-66.
- Kraus, H. (1980), *Creep Analysis*, John Wiley & Sons, New York, USA.
- Loghman, A. and Wahab, M.A. (1996), “Creep damage simulation of thick-walled tubes using the θ projection concept”, *Int. J. Press. Ves. Pip.*, **67**(1), 105-111.
- Loghman, A. and Shokouhi, N. (2009), “Creep damage evaluation of thick-walled spheres using a long-term creep constitutive model”, *J. Mech. Sci. Tech.*, **23**(10), 2577-2582.
- Loghman, A., Ghorbanpour Arani, A., Amir, S. and Vajedi, A. (2010), “Magnetothermoelastic creep analysis of functionally graded cylinders”, *Int. J. Press. Ves. Pip.*, **87**(7), 389-395.
- Loghman, A., Askari Kashan, A., Younesi Bidgoli, M., Shajari, A.R. and Ghorbanpour Arani, A. (2013), “Effect of particle content, size and temperature on magneto-thermo-mechanical creep behavior of composite cylinders”, *J. Mech. Sci. Tech.*, **27**(4), 1041-1051.
- Loghman, A., Nasr, M. and Arefi, M. (2017), “Non-symmetric thermomechanical analysis of a functionally graded cylinder subjected to mechanical, thermal, and magnetic loads”, *J. Therm. Stress.*, **40**(6), 1-18.
- Meziane, M.A.A., Abdelaziz, H.H. and Tounsi, A. (2014), “An efficient and simple refined theory for buckling and free vibration of exponentially graded sandwich plates under various boundary conditions”, *J. Sandw. Struct. Mater.*, **16**(3), 293-318.
- Mohammadimehr, M., Rostami, R. and Arefi, M. (2016), “Electro-elastic analysis of a sandwich thick plate considering FG core and composite piezoelectric layers on Pasternak foundation using TSDT”, *Steel Compos. Struct., Int. J.*, **20**(3), 513-543.
- Moosaie, A. (2016), “A nonlinear analysis of thermal stresses in an incompressible functionally graded hollow cylinder with temperature-dependent material properties”, *Eur. J. Mech. -A/Solids*, **55**, 212-220.
- Mouffoki, A., Adda Bedia, E.A., Houari, M.S.A., Tounsi, A. and Mahmoud, S.R. (2017), “Vibration analysis of nonlocal advanced nanobeams in hygro-thermal environment using a new two-unknown trigonometric shear deformation beam theory”, *Smart Struct. Syst., Int. J.*, **20**(3), 369-383.
- Penny, R.K. and Marriott, D.L. (1971), *Design for Creep*, McGraw-Hill, London and New York, USA.
- Rahimi, G.H., Arefi, M. and Khoshgoftar, M.J. (2012), “Electro elastic analysis of a pressurized thick-walled functionally graded piezoelectric cylinder using the first order shear deformation theory and energy method”, *Mechanika*, **18**(3), 292-300.
- Rimrott, F.P.J., Mills, E.J. and Marin, J. (1960), “Prediction

- of creep failure time for pressure vessels”, *J. Appl. Mech.*, **27**(2), 303-308.
- Sahan, M.F. (2015), “Transient analysis of cross-ply laminated shells using FSDT: Alternative formulation”, *Steel Compos. Struct., Int. J.*, **18**(4), 889-907.
- Sim, R.G. and Penny, R.K. (1971), “Plane strain creep behavior of thick-walled cylinders”, *Int. J. Mech. Sci.*, **13**(12), 987-1009.
- Tutuncu, N. and Ozturk, M. (2001), “Exact Solution for Stresses in Functionally Graded Pressure Vessels”, *Compos.: Part B (Eng)*, **32**(8), 683-686.
- Xuan, F.Z., Chen, J.J., Wang, Z. and Tu, S.T. (2009), “Time-dependent deformation and fracture of multi-material systems at high temperature”, *Int. J. Press. Ves. Pip.*, **86**(9), 604-615.
- Yahia, S.A., Atmane, H.A., Houari, M.S.A. and Tounsi, A. (2015), “Wave propagation in functionally graded plates with porosities using various higher-order shear deformation plate theories”, *Struct. Eng. Mech., Int. J.*, **53**(6), 1143-1165.
- Yang, Y.Y. (2000), “Time-dependent stress analysis in functionally graded materials”, *Int. J. Solid Struct.*, **37**(51), 7593-7608.
- You, L.H., Ou, H. and Zheng, Z.Y. (2007), “Creep deformations and stresses in thick-walled cylindrical vessels of functionally graded materials subjected to internal pressure”, *Compos. Struct.*, **78**(2), 285-291.
- Zemri, A., Houari, M.S.A., Bousahla, A.A. and Tounsi, A. (2015), “A mechanical response of functionally graded nanoscale beam: An assessment of a refined nonlocal shear deformation theory beam theory”, *Struct. Eng. Mech., Int. J.*, **54**(4), 693-710.
- Zenkour, A.M. and Arefi, M. (2017), “Nonlocal transient electrothermomechanical vibration and bending analysis of a functionally graded piezoelectric single-layered nanosheet rest on visco-Pasternak foundation”, *J. Therm. Stress.*, **40**(2), 167-184.

CC

Nomenclature

r	Radius of an arbitrary layer of cylinder
z	Coordinate of arbitrary layer of cylinder respect to middle surface
R	Radius of mid-surface of cylinder
W_x	Axial component of deformation
U_r	Radial component of deformation
u	Displacement component of axial deformation
w	Displacement component of radial deformation
ϕ_x	Rotational component of axial deformation
ϕ_r	Rotational component of radial deformation
ε_x	Axial strain
ε_z	Radial strain
ε_θ	Circumferential strain
ε_{xz}	Shear strain in xz plane
σ_{xx}	Axial stress
σ_{zz}	Radial stress
$\sigma_{\theta\theta}$	Circumferential stress
τ_{xz}	Shear stress
α	Heat expansion coefficient
E_i	Modulus of elasticity at the inner radius
$\dot{\varepsilon}_e$	The effective creep strain rate
σ_e	The effective stress
$\dot{\varepsilon}_r$	Creep strain rate in radial direction
$\dot{\varepsilon}_x$	Creep strain rate in axial direction
$\dot{\varepsilon}_\theta$	Creep strain rate in tangential direction
$\dot{\varepsilon}_{\gamma x}$	Creep strain rate in shear direction
h	Thickness of cylinder
U	Total energy
n, m_3	Non homogeneous index
$U_s(x)$	Mechanical strain energy
$f_i(x)$	A function of component of displacement and rotation
$A_i(x)$	General property of material
E	Modulus of elasticity
$P_i(x)$	Variable internal pressure
$P_o(x)$	Variable external pressure
$G_i, i = 1, 2, 3$	Matrix of coefficient
W	External work(due to pressure)
F	general potential function
$F(u, w, \phi_x, \phi_r, x)$	Functional of the system
$\{X\}$	Vector of general deformation
$\{F\}$	Vector of general force (thermal and mechanical)
R_i	Inner radius
R_o	Outer radius
m_i	Eigen values
T	Temperature distribution
\bar{u}	Energy per unit volume

dV	Element of volume
$B(r)$ & $n(r)$	Radial dependent creep parameter
$\dot{\epsilon}_r$	Total radial creep
$\dot{\epsilon}_x$	Total axial creep
$\dot{\epsilon}_\theta$	Total tangential creep
$\dot{\epsilon}_{rx}$	Total shear creep

Appendix A

$$G_1 = \begin{bmatrix} 2(1-\nu)A_1 & 2(1-\nu)A_2 & 0 & 0 \\ 2(1-\nu)A_2 & 2(1-\nu)A_3 & 0 & 0 \\ 0 & 0 & K(1-2\nu)A_1 & K(1-2\nu)A_2 \\ 0 & 0 & K(1-2\nu)A_2 & K(1-2\nu)A_3 \end{bmatrix}$$

$$G_2 = \begin{bmatrix} 0 & 0 & 2\nu A_4 & 2\nu(A_1 + A_6) \\ 0 & 0 & -K(1-2\nu)A_1 + 2\nu A_6 & -K(1-2\nu)A_2 + 2\nu(A_2 + A_9) \\ -2\nu A_4 & K(1-2\nu)A_1 - 2\nu A_6 & 0 & 0 \\ -2\nu(A_1 + A_6) & K(1-2\nu)A_2 - 2\nu(A_2 + A_9) & 0 & 0 \end{bmatrix}$$

$$G_3 = \begin{bmatrix} 0 & 0 & 0 & 0 \\ 0 & -K(1-2\nu)A_1 & 0 & 0 \\ 0 & 0 & -2(1-\nu)A_5 & -[2(1-\nu)A_7 + 2\nu A_4] \\ 0 & 0 & -[2(1-\nu)A_7 + 2\nu A_4] & -[2(1-\nu)(A_1 + A_8) + 4\nu A_6] \end{bmatrix}$$

$$F_1 = \mu_1 C_1 (n_0 - 1) \sigma_e^{n_0 - 2} \frac{\partial \sigma_e}{\partial x} [2\sigma_{xx} - (\sigma_{rr} + \sigma_{\theta\theta})]$$

$$+ \mu_1 C_1 \sigma_e^{n_0 - 1} \left[2 \frac{\partial \sigma_{xx}}{\partial x} - \left(\frac{\partial \sigma_{rr}}{\partial x} + \frac{\partial \sigma_{\theta\theta}}{\partial x} \right) \right]$$

$$F_2 = -3K \mu_1 C_1 \sigma_e^{n_0 - 1} \tau_{rx} + \mu_1 C_2 (n_0 - 1) \sigma_e^{n_0 - 2} \frac{\partial \sigma_e}{\partial x} [2\sigma_{xx} - (\sigma_{rr} + \sigma_{\theta\theta})]$$

$$+ \mu_1 C_2 \sigma_e^{n_0 - 1} \left[2 \frac{\partial \sigma_{xx}}{\partial x} - \left(\frac{\partial \sigma_{rr}}{\partial x} + \frac{\partial \sigma_{\theta\theta}}{\partial x} \right) \right]$$

$$F_3 = 3K \mu_1 C_1 \left[(n_0 - 1) \sigma_e^{n_0 - 2} \frac{\partial \sigma_e}{\partial x} \tau_{rx} + \sigma_e^{n_0 - 1} \frac{\partial \tau_{rx}}{\partial x} \right]$$

$$+ \mu_1 C_3 \sigma_e^{n_0 - 1} [2\sigma_{\theta\theta} - (\sigma_{rr} + \sigma_{xx})]$$

$$F_4 = +3K \mu_1 C_2 \left[(n_0 - 1) \sigma_e^{n_0 - 2} \frac{\partial \sigma_e}{\partial x} \tau_{rx} + \sigma_e^{n_0 - 1} \frac{\partial \tau_{rx}}{\partial x} \right]$$

$$- \mu_1 [C_1 [2\sigma_{rr} - (\sigma_{\theta\theta} + \sigma_{xx})] + C_4 [2\sigma_{\theta\theta} - (\sigma_{rr} + \sigma_{xx})]]$$